

# X-ray Groups of Galaxies at $0.5 < z < 1$ in zCOSMOS: Increased AGN Activities in High Redshift Groups

M. TANAKA<sup>1</sup>, A. FINOGUENOV<sup>2</sup>, S. J. LILLY<sup>3</sup>, M. BOLZONELLA<sup>11</sup>, C. M. CAROLLO<sup>3</sup>, T. CONTINI<sup>4,5</sup>, A. IOVINO<sup>6</sup>,  
J.-P. KNEIB<sup>7</sup>, F. LAMAREILLE<sup>4,5</sup>, O. LE FEVRE<sup>7</sup>, V. MAINIERI<sup>8</sup>, V. PRESOTTO<sup>6</sup>, A. RENZINI<sup>9</sup>, M. SCODEGGIO<sup>10</sup>,  
J. D. SILVERMAN<sup>1</sup>, G. ZAMORANI<sup>11</sup>, S. BARDELLI<sup>11</sup>, A. BONGIORNO<sup>2</sup>, K. CAPUTI<sup>12</sup>, O. CUCCIATI<sup>6</sup>, S. DE LA TORRE<sup>12</sup>,  
L. DE RAVEL<sup>12</sup>, P. FRANZETTI<sup>10</sup>, B. GARILLI<sup>10</sup>, P. KAMPCZYK<sup>3</sup>, C. KNOBEL<sup>3</sup>, K. KOVAČ<sup>3,13</sup>, J.-F. LE BORGNE<sup>4,5</sup>, V. LE  
BRUN<sup>7</sup>, C. LÓPEZ-SANJUAN<sup>7</sup>, C. MAIER<sup>3</sup>, M. MIGNOLI<sup>11</sup>, R. PELLO<sup>4,5</sup>, Y. PENG<sup>4,5</sup>, E. PEREZ MONTERO<sup>4,5,14</sup>, L. TASCA<sup>7</sup>,  
L. TRESSE<sup>7</sup>, D. VERGANI<sup>11</sup>, E. ZUCCA<sup>11</sup>, L. BARNES<sup>3</sup>, R. BORDOLOI<sup>3</sup>, A. CAPPI<sup>11</sup>, A. CIMATTI<sup>15</sup>, G. COPPA<sup>2</sup>,  
A. M. KOEKEMOER<sup>16</sup>, H. J. MCCracken<sup>17</sup>, M. MORESCO<sup>15</sup>, P. NAIR<sup>11</sup>, P. OESCH<sup>3</sup>, L. POZZETTI<sup>11</sup>, N. WELIKALA<sup>18</sup>

<sup>1</sup>*Institute for the Physics and Mathematics of the Universe, The University of Tokyo, 5-1-5 Kashiwanoha, Kashiwa-shi, Chiba 277-8583, Japan*  
<sup>2</sup>*Max-Planck Institut für extraterrestrische Physik, Giessenbachstrasse, D-85748 Garching bei München, Germany*  
<sup>3</sup>*Institute of Astronomy, ETH Zürich, Zürich 8093, Switzerland*  
<sup>4</sup>*Institut de Recherche en Astrophysique et Planétologie, CNRS, 14, avenue Edouard Belin, F-31400 Toulouse, France*  
<sup>5</sup>*IRAP, Université de Toulouse, UPS-OMP, Toulouse, France*  
<sup>6</sup>*INAF Osservatorio Astronomico di Brera, Milan, Italy*  
<sup>7</sup>*Laboratoire d'Astrophysique de Marseille, CNRS/Aix-Marseille Université, 38 rue Frédéric Joliot-Curie, 13388, Marseille cedex 13, France*  
<sup>8</sup>*European Southern Observatory, Karl-Schwarzschild-Str. 2, D-85748 Garching bei München, Germany*  
<sup>9</sup>*Dipartimento di Astronomia, Università di Padova, Padova, Italy*  
<sup>10</sup>*INAF - IASF Milano, Milan, Italy*  
<sup>11</sup>*INAF Osservatorio Astronomico di Bologna, Bologna, Italy*  
<sup>12</sup>*Institute for Astronomy, University of Edinburgh, Royal Observatory, Blackford Hill, Edinburgh EH9 3HJ, UK*  
<sup>13</sup>*Max-Planck Institut für Astrophysik, D-85748, Garching bei München, Germany*  
<sup>14</sup>*Instituto de Astrofísica de Andalucía, CSIC, Apartado de correos 3004, 18080 Granada, Spain*  
<sup>15</sup>*Dipartimento di Astronomia, Università degli Studi di Bologna, Bologna, Italy*  
<sup>16</sup>*Space Telescope Science Institute, Baltimore, Maryland 21218, USA*  
<sup>17</sup>*Institut d'Astrophysique de Paris, UMR7095 CNRS, Université Pierre & Marie Curie, 75014 Paris, France*  
<sup>18</sup>*Insitut d'Astrophysique Spatiale, CNRS & Universit de Paris Sud-XI, 91405 Orsay Cedex, France*

(Received ; accepted )

## Abstract

We present a photometric and spectroscopic study of galaxies at  $0.5 < z < 1$  as a function of environment based on data from the zCOSMOS survey. There is a fair amount of evidence that galaxy properties depend on mass of groups and clusters, in the sense that quiescent galaxies prefer more massive systems. We base our analysis on a mass-selected environment using X-ray groups of galaxies and define the group membership using a large number of spectroscopic redshifts from zCOSMOS. We show that the fraction of red galaxies is higher in groups than in the field at all redshifts probed in our study. Interestingly, the fraction of [OII] emitters on the red sequence increases at higher redshifts in groups, while the fraction does not strongly evolve in the field. This is due to increased dusty star formation activities and/or increased activities of active galactic nuclei (AGNs) in high redshift groups. We study these possibilities using the 30-band photometry and X-ray data. We find that the stellar population of the red [OII] emitters in groups is old and there is no clear hint of dusty star formation activities in those galaxies. The observed increase of red [OII] emitters in groups is likely due to increased AGN activities. However, our overall statistics is poor and any firm conclusions need to be drawn from a larger statistical sample of  $z \sim 1$  groups.

**Key words:** surveys, galaxies: evolution, galaxies: fundamental parameters, galaxies: clusters: general

## 1. Introduction

The matter distribution in the early universe is nearly uniform, but not completely so, and small density fluctuations grow with time through gravitational forces. Eventually, matter becomes dense enough to initiate star formation and galaxies form in high density peaks of the density fluctuations. Galaxies grow progressively more massive by accreting material from the surroundings and by merging with other galaxies. The cosmic large-scale structure, in which galaxies are embedded, also

develops with time. Later, clusters of galaxies form at the nodes of filaments, where galaxies can be quenched by gravitational and gas-dynamical effects. The evolution of galaxies and large-scale structure goes in tandem and galaxies eventually acquire the properties that we observe today. This current framework of galaxy formation and evolution indicates that the formation and evolution of galaxies are driven by statistical events (e.g., they form in density fluctuations and grow by mergers) and galaxies are statistical objects in nature. They do not form at the same time and they do not evolve in the same

way. Only by statistical analyses can we study the physics of galaxy formation and evolution.

This fundamental principle has motivated a number of galaxy surveys. Imaging surveys deliver limited information about galaxy properties because one needs precise distances to galaxies in order to translate observed quantities into physical quantities. For this reason, several large spectroscopic surveys have been carried out to date and they have brought new insights into galaxy evolution over cosmological time scales.

The CfA redshift survey carried out the first systematic spectroscopic survey of the local universe in the late-70's (Geller & Huchra 1989). They measured redshifts of nearby galaxies and revealed the cosmic large-scale structure in the local universe, making a major progress in our understanding of galaxy distribution in the universe. Following the CfA redshift survey, the Las Campanas redshift survey (Shectman et al. 1996) mapped out the galaxy distribution out to larger distances, and the Canada-France redshift survey (Lilly et al. 1995) reached out to  $z = 1$ . The Sloan Digital Sky Survey (SDSS; York et al. 2000) and the 2 degree field redshift survey (2dF; Colless et al. 2003) surpassed the previous surveys with much improved statistics. In particular, SDSS imaged a quarter of the sky in five photometric bands (Fukugita et al. 1996; Doi et al. 2010) and measured more than 2 million redshifts with unprecedented precision (Aihara et al. 2011). The SDSS dramatically refined our view of the local universe. In parallel to these surveys of the local universe, large spectroscopic surveys with 8m telescopes such as DEEP2 (Davis et al. 2003), VIMOS VLT Deep Survey (Le Fèvre et al. 2005), and zCOSMOS (Lilly et al. 2007) peered deep into the universe reaching  $z > 1$ . All of these surveys enabled statistical analyses of galaxy populations over a large redshift range, bringing in new insights into the evolution of galaxies. This paper is in a context of such statistical galaxy studies from large spectroscopic surveys. We will study galaxy properties out to  $z = 1$  using data from zCOSMOS with a particular emphasis on the dependence of galaxy properties on environment.

A pioneering work on this subject was made by Dressler (1980), who first quantified the morphology-density relation. Following this work, many authors studied the relationship between galaxy properties and environment (e.g., Postman & Geller 1984; Whitmore et al. 1993; Balogh et al. 1997; Dressler et al. 1997; Poggianti et al. 1999; see Tanaka et al. 2005 for a thorough set of references and also see below for more recent papers). The SDSS and 2dF data sets delivered the unprecedented statistics and we now have a fairly good understanding of galaxy properties in the local universe (Lewis et al. 2002; Gómez et al. 2003; Blanton et al. 2003; Goto et al. 2003; Kauffmann et al. 2004; Tanaka et al. 2004; Blanton et al. 2005; Baldry et al. 2006). The advent of 8m-class telescopes pushed those environment studies to redshift of unity and beyond (Rosati et al. 1999; Kodama et al. 2001; Lubin et al. 2002; Demarco et al. 2005; Nakata et al. 2005; Poggianti et al. 2006; Stanford et al. 2005; Tanaka et al. 2005; Stanford et al. 2006; Demarco et al. 2007; Koyama et al. 2007; Fassbender et al. 2008; Lidman et al. 2008; Poggianti et al. 2008; Mei et al. 2009; Bauer et al. 2011; Rettura et al. 2010; Strazzullo et al. 2010; Tanaka et al. 2010a; Tanaka et al. 2010b). However, many of these high- $z$  studies still suffer from limited statistics

particularly in low-medium density environments and this is the area where large spectroscopic surveys fill in as they mainly probe such environments (Cucciati et al. 2006; Cooper et al. 2007; Tasca et al. 2009; Bolzonella et al. 2010; Cucciati et al. 2010; Cooper et al. 2010; Iovino et al. 2010).

However, results from these deep surveys and their interpretations are not always consistent. In particular, the dependence of galaxy colors on environment at  $z \sim 1$  is controversial as discussed in Cooper et al. (2010). There are a number of differences between the data sets from different surveys and the ways the analyses are made, which might explain the possible inconsistency. In this paper, we study photometric and spectroscopic properties of galaxies as a function of environment and make an attempt to settle the issue. A unique feature of our study is that we define mass-selected environments using X-ray groups. Most of the previous studies are based on environment traced by galaxies and there is room for observational biases to come in. Such biases include sampling rate, redshift success rate as functions of redshift and galaxy type, large-scale structure, etc. For example, if a sample is biased towards star forming galaxies, which can be the case at high redshifts in optical surveys, the density field traced by galaxies is basically the density of star forming galaxies, which may not represent the true density field. X-rays, on the other hand, are free from such biases. An extended X-ray emission is a strong signature of a dynamically bound system. Also, an X-ray luminosity is a good proxy for mass of a system, making it possible to define environments by mass. We present a robust analysis of the dependence of galaxy properties on environment based on stellar mass limited galaxy sample with mass-selected environments.

The structure of this paper is as follows. We briefly summarize the zCOSMOS survey and construct an X-ray group catalog in Section 2. We then study properties of the group galaxies and make comparisons to field galaxies in Section 3. Section 4 discusses the results and the paper is concluded in Section 5. Unless otherwise stated, we use  $\Omega_M = 0.26$ ,  $\Omega_\Lambda = 0.74$ , and  $H_0 = 72 \text{ km s}^{-1} \text{ Mpc}^{-1}$ . The uncertainties are given in 68% confidence intervals. All the magnitudes are given in the AB system.

## 2. X-ray Group and Member Galaxy Catalogs

We study spectroscopic properties of galaxies up to  $z = 1$  based on data from the zCOSMOS survey (Lilly et al. 2007). We first briefly describe the survey and move on to construct a catalog of galaxy groups selected from deep X-ray data.

### 2.1. The zCOSMOS redshift survey

The zCOSMOS survey is a spectroscopic survey of the COSMOS field (Scoville et al. 2007; Koekemoer et al. 2007) using the VIMOS spectrograph on the Very Large Telescope on the Cerro Paranal (Le Fèvre et al. 2003). It is the largest program ever conducted at VLT with 600 hours of allocated time. The survey consists of two components: zCOSMOS-bright and zCOSMOS-faint. The former is a flux-limited survey down to  $I_{AB} = 22.5$  using the medium resolution grism ( $R \sim 500$ ) with a wavelength coverage of  $5550 - 9650 \text{ \AA}$ . The latter is a color-selected galaxy survey aiming at  $z \sim 2$  galaxies using the low-resolution blue grism with  $R \sim 200$  over  $3700 - 6700 \text{ \AA}$ .

All the spectra are visually inspected by two people independently and final redshifts and confidence flags are determined through face-face reconciliation meetings. In this study, we use the zCOSMOS-bright 20k data to perform statistical analysis of galaxy groups. For further details of the survey, the readers are referred to Lilly et al. (2007) and Lilly et al. (2009).

## 2.2. X-ray group catalog

We construct an X-ray group catalog using X-ray data from XMM-Newton and Chandra available in the COSMOS field (Hasinger et al. 2007; Elvis et al. 2009). An early version of the group catalog was presented in Finoguenov et al. (2007), in which we relied only on photometric redshifts to identify the optical counterparts of extended X-ray emission. We revise the catalog with an efficient group identification algorithm demonstrated by Bielby et al. (2010) and Finoguenov et al. (2010) to the massive COSMOS data set. We give the full details in Finoguenov et al. (in prep), and here we only briefly outline our algorithm.

On the mosaic of coadded XMM and Chandra images, cluster candidates are first identified as extended sources through a classical wavelet transform technique with a careful removal of point sources (Finoguenov et al. 2009). Next, we look for the cluster red sequence around the extended X-ray sources using the deep optical-IR data. For this red sequence search, we construct model red sequence using the recipe by Lidman et al. (2008) and quantify a significance of red sequence around an extended X-ray source at a given redshift in the following manner:

- We extract galaxies located within 1 Mpc (physical) from the X-ray center and have  $|z_{phot} - z| < 0.1$ , where  $z_{phot}$  is the photometric redshift of a galaxy and  $z$  is the redshift at which we want to quantify the red sequence.
- We count galaxies with weights according to their spatial locations from the X-ray center and to their location on a color-magnitude diagram. Bright red galaxies located at the center have the highest weight.
- We compare the count with the average count and its dispersion, which are derived by placing the apertures of the same size at random positions in the COSMOS field, to quantify the significance of the red sequence.
- We repeat the above procedure at  $0 < z < 2.5$  to identify peaks of the red sequence signals.
- Finally, we visually inspect all the significant peaks and assign redshift and confidence flag to the X-ray source.

In the first procedure, we make use of the excellent photometric redshift in the COSMOS field (Ilbert et al. 2009) to efficiently eliminate fore-/background contamination. In the second step, we change the filter combinations to compute colors with redshift. We have to make a compromise between the depth of the data and filter combinations to probe similar rest-frame wavelengths at different redshifts, but we always straddle the 4000Å break, which is a sensitive feature to star formation. To be specific, we use the following color-magnitude diagrams.

- $0.0 < z < 0.3 : u - r$  vs.  $r$
- $0.3 < z < 0.6 : B - i$  vs.  $i$
- $0.6 < z < 1.0 : r - z$  vs.  $z$

- $1.0 < z < 1.5 : i - K_S$  vs.  $K_S$
- $1.5 < z < 2.5 : z - 3.6\mu m$  vs.  $3.6\mu m$

Finally, all the significant red sequence signals are visually inspected and the group redshifts and confidence flags are assigned. We use the 20k redshifts from zCOSMOS (Lilly et al. 2007) to help identify the systems and obtain spectroscopic redshifts of them in this final identification procedure. Details of the confidence flags will be described in Finoguenov et al. (in prep.), but in short, we give FLAG=1 to groups that are unambiguously confirmed with spectroscopic redshifts and the X-ray centroid is reliably determined by high significance X-ray fluxes. FLAG=2 is for spectroscopically confirmed groups whose X-ray center can potentially be off (up to 30 arcsec) due to low fluxes or to blending with other sources, and the location of the optical counterparts were used in the centroid determinations. We have confirmed that these uncertain centroids do not affect our results as we discuss below. FLAG=3 groups are likely real groups but they are not spectroscopically confirmed yet. The catalog contains 215 groups with FLAG=1, 2 or 3, of which 195 are at  $z < 1$ . We note that  $\sim 90\%$  (175 out of 195) of the groups at  $z < 1$  are spectroscopically confirmed (i.e., FLAG=1 or 2). We do not use those FLAG=3 groups in this work, but we have confirmed that our results do not change if we include them.

## 2.3. Group members from zCOSMOS

We define the group membership using the X-ray group catalog constructed above and the spectroscopic redshifts from zCOSMOS. In this work, we apply the following selection criteria to study the dependence of galaxy properties on environment:

1. We use spectroscopically confirmed groups at  $0.5 < z < 1.0$  with masses between  $3 \times 10^{13} M_\odot$  and  $7 \times 10^{13} M_\odot$ .
2. We define group members as galaxies with high confidence spectroscopic redshifts from zCOSMOS and located within  $< 2\sigma$  and  $< R_{200}$  from the group centers, where  $\sigma$  is line-of-sight velocity dispersion and  $R_{200}$  is a virial radius of a group within which the mean interior density is 200 times the critical density of the universe at the group redshift.

The first criterion is about groups themselves. We want to reduce spurious groups that contaminate the analysis. For this, we use groups with flag 1 or 2. As mentioned above, they are spectroscopically confirmed groups. We then restrict the sample to  $0.5 < z < 1.0$  as shown in Fig. 1. This redshift selection is motivated to have the [OII] emission in our spectral coverage. The line is not available at  $z < 0.5$  and we could in principle use H $\alpha$  to fill that redshift range. But, these two lines have different sensitivities to star formation and AGN (e.g., H $\alpha$  is much more robust to extinction) and it is hard to make fair comparisons between [OII] emitters and H $\alpha$  emitters. We do not include the  $z < 0.5$  groups in order to perform a robust analysis. We do not include  $z > 1$  groups either as extremely strong fringes in the VIMOS spectra decrease the success rate of obtaining redshifts of passive galaxies at  $z > 1$ , making any spectral analysis at  $z > 1$  difficult.

In addition to the redshift criterion, we impose a group mass threshold. As shown by previous studies (e.g., Tanaka et al.



2005; Poggianti et al. 2006; Koyama et al. 2007), galaxy properties depend on group mass. In order to eliminate any strong group mass dependence and extract evolutionary trends, we use groups with masses ( $M_{200}$ , which is the mass contained within  $R_{200}$ ) between  $3 \times 10^{13} M_{\odot}$  and  $7 \times 10^{13} M_{\odot}$  as shown in Figure 1. Note that  $M_{200}$  is derived from the X-ray scaling relation calibrated against weak lensing mass estimates (Leauthaud et al. 2010). We still have a weak mass tendency within the narrow mass range in the sense that we tend to have more massive systems at higher redshifts. This bias *weakens* any evolutionary trends because more massive groups tend to be more evolved. If we had a flat group mass distribution at  $0.5 < z < 1.0$ , we would have observed stronger evolutionary trends than those shown below.

The second criterion is the definition of group members. In this work, we use galaxies with highly confident spectroscopic redshifts from zCOSMOS. Specifically, we use galaxies with flags 4's, 3's (including 14's and 13's), 2.5, 2.4, 9.5, 9.4, and 9.3. For details of the flags, readers are referred to Lilly et al. (2009).

To define the group membership, we first estimate  $M_{200}$  from the X-rays. From this, we evaluate the velocity dispersions ( $\sigma$ ) and virial radii ( $R_{200}$ ) of the groups assuming that they are virialized (Carlberg et al. 1997). As most group galaxies are observed to lie within  $\sim R_{200}$  in the local universe (Gómez et al. 2003; Tanaka et al. 2004), we define group members as those within  $< R_{200}$  from the centers. The centers of groups with FLAG=2 can be uncertain, but this is not a major concern in our analysis because a typical  $R_{200}$  of these groups is 2.5 times larger than the maximum positional uncertainty of 30 arcsec. We have checked the robustness of our results by perturbing the centers of the FLAG=2 groups with a Gaussian function with  $\sigma = 30$  arcsec and repeated all the analysis in this paper. We have observed no appreciable changes in our results. For the line-of-sight separation, we apply  $< 2\sigma$  from the redshift centers of the groups. Galaxies that do not belong to any groups are defined as field galaxies. In total, we have 7,549 galaxies with high confidence redshifts at  $0.5 < z < 1$ , of which 246 are in groups satisfying the criteria above. We will further apply a stellar mass cut to the galaxies in the next section, and the total numbers of galaxies used in the main analyses are 1,574 and 96 for the field and group environments, respectively.

### 3. Galaxy Populations in the X-ray Groups at $0.5 < z < 1.0$

#### 3.1. Color-mass diagram and the fraction of red galaxies

We base our analysis on the group catalog and member catalog constructed in the last section and study properties of galaxies as functions of redshift and environment (i.e., group vs. field). To give an overview of the properties of galaxies in our catalog, we show a rest-frame  $u - r$  color vs. stellar mass diagram in Fig. 2. The rest-frame color and stellar mass are derived by Bolzonella et al. (2010) by fitting the photometry with model templates from Bruzual & Charlot (2003) assuming the Chabrier initial mass function (Chabrier 2003). A typical error in our stellar mass estimates is  $\sim 0.2$  dex (see Bolzonella et al. 2010 for details). Before we discuss the plot, let us introduce

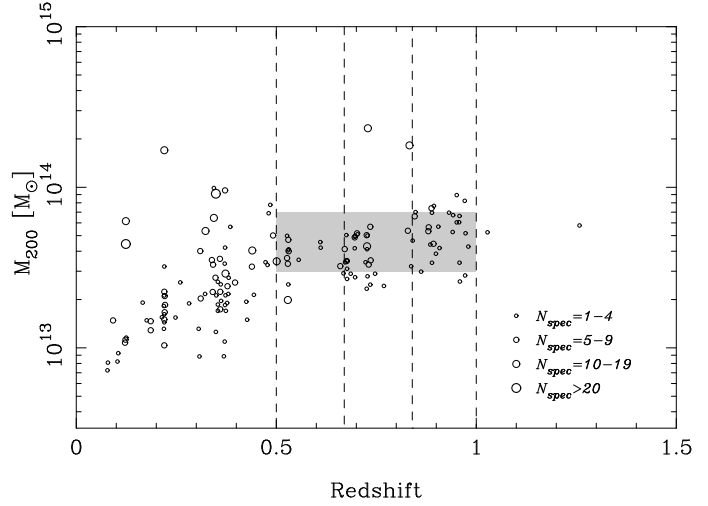


**Fig. 1.**  $M_{200}$  of groups measured from X-rays plotted against redshift. We use groups with high confidence flags only. We make three redshift bins ( $0.5 < z < 0.67$ ,  $0.67 < z < 0.84$ , and  $0.84 < z < 1.00$ ) as indicated by the vertical dashed lines, where we have the [OII] line in the spectral wavelength coverage and we are not strongly affected by fringes in the spectra. In order to minimize the group mass dependence of galaxy properties, we use a narrow mass range as shown by the shade in this work. The sizes of the symbols correlate with the number of spectroscopic members.

our definition of (a) red/blue galaxies and (b) [OII] emitters.

(a) We divide galaxies into red and blue galaxies by their rest-frame  $u - r$  color. We perform a biweight fit to the red sequence in groups at  $0.67 < z < 0.85$ , where we observe the most prominent red sequence due to the largest number of group galaxies we have there. We then shift it by  $\Delta(u - r) = -0.3$  shown as the slanted dashed line in Fig. 2 to separate the two populations. The amount of the shift is motivated to give a reasonable separation between [OII] emitters and non-[OII] emitters (see below for their definitions). We have confirmed that our conclusions are insensitive to a small change in the amount of the shift. We correct for the color evolution of the red sequence in the other bins using an instantaneous burst model formed at  $z_f = 3$  from Bruzual & Charlot (2003). As seen in the figure, the color threshold is bluer at higher redshift.

(b) We also use [OII] emission to characterize galaxy properties. We use the equivalent widths of [OII] measured by Lamareille et al. (in prep). Line detections below  $1.15\sigma$  are considered fake and here we adopt a conservative significance threshold of  $2.3\sigma$  to ensure that the line is securely detected. We define galaxies with  $\text{EW}[\text{OII}] < -5\text{\AA}$  detected at  $> 2.3\sigma$  as [OII] emitters, and the other galaxies as quiescent. Note we use a negative sign for emission.

Going back to Fig. 2, it is immediately clear that the most massive galaxies tend to be red and many of them do not show a sign of active star formation. Galaxies with no significant [OII] form a clear sequence of red galaxies. Interestingly, some of the red galaxies show significant [OII] emissions despite their red colors. In contrast to massive galaxies, low-mass galaxies are predominantly blue [OII] emitters. This is due to a bias introduced by the flux limit of the survey. The  $I$ -band, with

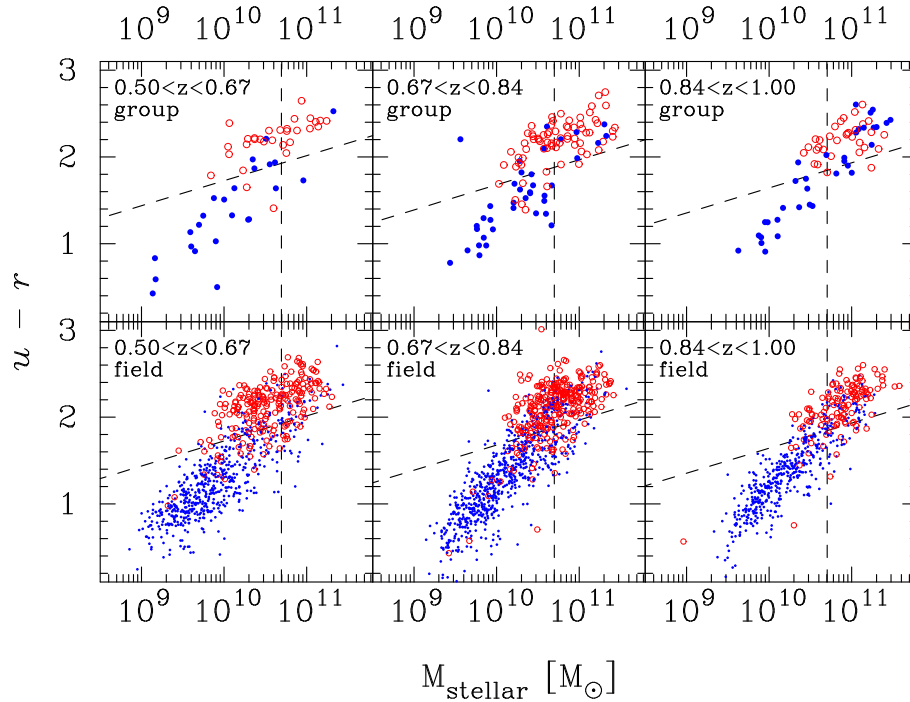


**Fig. 2.** Rest-frame  $u - r$  color plotted against stellar mass. The top panels show the group galaxies and the bottom panels show the field galaxies. The panels are split in three redshift bins. The filled and open symbols show galaxies with and without significant [OII] emission ( $\text{EW}[\text{OII}] < -5\text{\AA}$  at  $> 2.3\sigma$ ), respectively. The vertical dashed lines are our mass threshold, which defines the stellar mass limited galaxy sample. We separate red and blue galaxies using the slanted dashed line. For clarify, we plot only one third of the field galaxies.

which spectroscopic targets are selected in zCOSMOS, samples bluer light in rest-frame at higher redshifts, and we are missing low-mass red galaxies, resulting in a strong bias towards blue, star forming galaxies.

It is hard to interpret Fig. 2 due to the strong selection bias. We apply a stellar mass cut in each redshift bin to construct a stellar mass limited sample in order to study evolutionary trends. We have to correct for the mass evolution in each redshift bin, but we cannot track the mass evolution of individual galaxies, which depends on their star formation and merger histories. Here, we simply apply correction for the passive evolution using the same passive evolution model as used for the color evolution. We can reach  $\sim 5 \times 10^{10} M_{\odot}$  galaxies at  $z = 1$  in zCOSMOS, although the redshift success rate drops to 70% (see Figs 2 and 10 of Lilly et al. 2009). Cucciati et al. (2010) and Iovino et al. (2010) applied a conservative cut of  $10^{11} M_{\odot}$ , but for the purpose of the paper, we do not need to be 100% complete and we apply a stellar mass thresholds of  $4.95 \times 10^{10} M_{\odot}$ ,  $5 \times 10^{10} M_{\odot}$ , and  $5.05 \times 10^{10} M_{\odot}$  at  $0.5 < z < 0.67$ ,  $0.67 < z < 0.84$ , and  $0.84 < z < 1$ , respectively. We note that our conclusions do not change if we adopt a conservative mass cut of  $10^{11} M_{\odot}$ , although the statistics becomes poor. Balogh et al. (2011) reported on an abundant population of green valley galaxies in groups at  $0.85 < z < 1$ . We do not observe strong evidence for an increased amount of green galaxies in Fig. 2, but we cannot probe as low-mass galaxies as they did ( $10^{10.1} M_{\odot}$ ).

We plot the fraction of red galaxies as a function of redshift in Fig. 3 using the stellar mass limited sample. The fraction of massive red galaxies remains constant over the explored red-

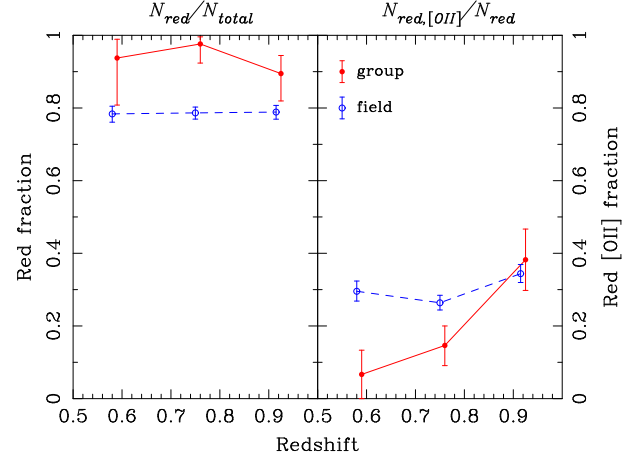


**Fig. 3.** **Left:** Fraction of red galaxies plotted against redshift. Here we use the stellar mass limited sample in both the group and field environments. The filled and open symbols are for the group and field samples, respectively. They are slightly shifted horizontally to avoid overlapping. The error bars show 68% confidence interval (Gehrels 1986). **Right:** Fraction of [OII] emitters among red galaxies against redshift.

shift range in both groups and field. An interesting trend in Fig. 3 is that the red fraction is always higher in groups than in the field, showing clear environmental dependence of galaxy colors at  $0.5 < z < 1$ . This may appear inconsistent with previous studies (e.g., Cucciati et al. 2010; Iovino et al. 2010), and we will discuss that in Section 4.1. While we do not see strong color evolution, we see a clear increase in the fraction of [OII] emitters among red galaxies at high redshifts as shown in the right panel of Fig. 3. As discussed earlier, our group sample is biased towards more massive groups at higher redshifts, which weakens any evolutionary trends. Also, due to the nature of a mass limited sample, spectra at higher redshifts are of lower signal-to-noise ratios. We tend to miss weak [OII] emissions at higher redshifts, which weakens the trend we see here<sup>1</sup>. The real evolutionary trend should be stronger than that observed in Fig. 3.

The fraction of red [OII] emitters in the field remains nearly constant with redshift, while it evolves very fast in groups. The fractions become indistinguishable in between groups and field in the highest redshift bin. These red [OII] emitters must have dusty star formation activities and/or AGN activities. This is a sort of evolution that cannot be revealed by broad-band photometry, demonstrating a power of large spectroscopic surveys.

### 3.2. Stellar mass and redshift dependence of the [OII] emitters

Essentially all galaxy properties are correlated with stellar mass. It would be important to show that the higher red fraction in groups observed in Fig. 3 is not due to the environmental dependence of the stellar mass function such that groups host a larger fraction of massive galaxies, which increases the red fraction because massive galaxies tend to be red. We plot in Fig. 4 the fraction of red galaxies as functions of stellar mass and redshift. We find that the red fraction tends to be higher in groups than in the field at a given stellar mass, although the error bars often overlap. The difference between groups and field is particularly clear at  $0.67 < z < 0.84$ , where we have a prominent large-scale structure (Guzzo et al. 2007). The poor statistics does not allow us to conclude that the groups show a higher red fraction at a given stellar mass, but the systematically higher fraction suggests that the observed high red fraction in groups in Fig. 3 is not entirely due to the dependence of stellar mass function on environment. We note that George et al. (2011) showed that the red fraction is higher in groups than in the field at a given stellar mass based on the same X-ray group catalog and on the photometric data in COSMOS.

Similarly, it would be interesting to look at the stellar mass dependence of the [OII] emitters on the red sequence. We plot in Fig 5 the fraction of the red [OII] as a function of stellar mass. In the field, the fraction of the red [OII] emitters does not strongly depend on mass above the mass threshold. The

overall fraction does not show a strong increase with redshift either. On the other hand, the fraction in groups increases at higher redshift, and in the highest redshift bin, the fraction of [OII] emitters seems to increase with increasing mass above the mass cut. Although the statistics is poor, this is a contrasting trend to the field. It seems that the increase of [OII] emitters in groups at high redshift is stronger for more massive galaxies.

A high fraction of [OII] emitters at  $z \sim 1$  has already been observed by several authors. Nakata et al. (2005) found a fraction of  $\text{EW}[\text{OII}] < -10\text{\AA}$  galaxies of  $\sim 0.45 \pm 0.15$  at  $0.8 < z < 1$ . Their sample is not stellar mass limited and we cannot make a fair comparison with theirs. But, if we apply the same selection of  $\text{EW}[\text{OII}] < -10\text{\AA}$  to our sample, we obtain a consistent fraction of  $0.31 \pm 0.07$ . Poggianti et al. (2006) showed the high fraction (very roughly 50%) in groups and clusters at  $0.4 < z < 0.8$ . If we apply  $\text{EW}[\text{OII}] < -3\text{\AA}$  as done in Poggianti et al. (2006), we obtain a consistent fraction. A similarly high fraction of [OII] emitters in groups at higher redshift ( $z = 1.2$ ) is reported by Tanaka et al. (2009). If we apply our definition of [OII] emitters and the stellar mass cut to their sample, we find that the fraction of massive [OII] emitters is  $0.47 \pm 0.22$ . We should be careful with this face value as their sample was drawn from optically selected groups and the targets for spectroscopy were photo- $z$  selected, which potentially introduces biases in the sample. However, this high fraction of [OII] emitting galaxies in groups drawn from completely different sample is reassuring. Unfortunately, their sample is not large enough to constrain the mass dependence of the [OII] emitters.

Not only the fraction of red [OII] emitters, but strengths of the emission seem to increase with increasing redshift as shown in Fig. 6. Field galaxies do not show any strong change in the median  $\text{EW}[\text{OII}]$  with redshift. On the other hand, group galaxies seem to show a larger  $\text{EW}[\text{OII}]$  tail at higher redshifts. The distributions of  $\text{EW}[\text{OII}]$  in groups at  $0.67 < z < 0.84$  and  $0.84 < z < 1$  show a null probability of 3% from the Mann-Whitney  $U$  test. This increase in  $\text{EW}[\text{OII}]$  would not be too surprising given the rapid increase in the fraction of [OII] emitters observed in Fig. 3, which is statistically significant. We have only one red [OII] emitter at  $0.50 < z < 0.64$ , and we cannot apply any statistical tests there. In contrast to groups, field galaxies do not show any strong evolutionary trends: the Mann-Whitney test gives a null probability of 33% between  $0.50 < z < 0.64$  and  $0.67 < z < 0.84$ , and 47% between  $0.67 < z < 0.84$  and  $0.84 < z < 1$ . Wilman et al. (2008) showed that  $\sim 50\%$  of galaxies with  $10^{11} M_{\odot}$  in  $z \sim 0.4$  groups show infrared flux excess, which can be due to star formation and/or AGN. The observed low frequency of the [OII] emitters compared to the infrared detections may be because [OII] and infrared have different sensitivities to star formation and AGN. It could also be because of our conservative  $\text{EW}[\text{OII}]$  cut.

To summarize, we observe that the fraction of red galaxies with  $> 5 \times 10^{10} M_{\odot}$  does not strongly evolve at  $0.5 < z < 1$  in both group and field environments, and it is always higher in groups than in the field. The most striking trend that we find is that the fraction of red [OII] emitters in groups increases at higher redshifts, while the fraction is nearly constant in the field. It seems that more massive galaxies in groups show stronger increase in [OII]. This trend suggests that the red galaxies in groups have dusty star formation and/or AGN ac-

<sup>1</sup> One might suspect that we tend to miss quiescent red galaxies at  $z \sim 1$  due to the busy OH lines, and that might be driving the observed increase of red galaxies with [OII] emission, which are easier to identify. However, as will be discussed in Section 3.2, red [OII] emitters increases with increasing stellar mass in the highest redshift bin. This is an opposite trend from what expected from the redshift determination bias because we do not miss massive (bright) passive galaxies even under the presence of busy OH lines. Therefore, the observed trend is unlikely due to an observational bias.

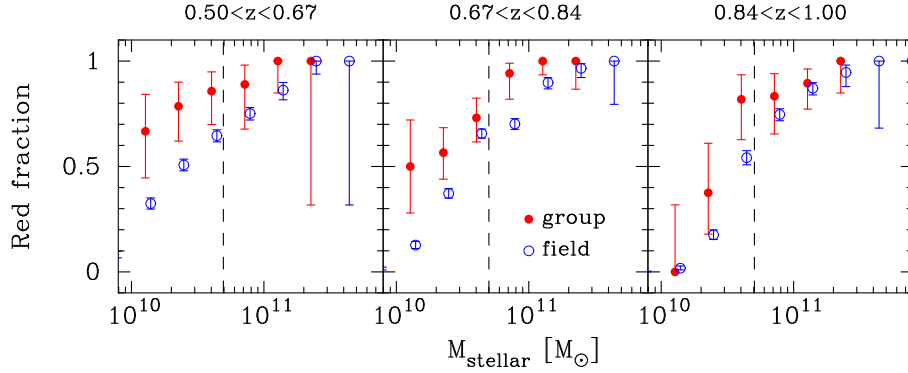


**Fig. 4.** Fraction of red galaxies as a function of stellar mass in the three redshift bins. The filled and open circles are the group and field galaxies, respectively. The vertical dashed lines are the mass thresholds, which define the stellar mass limited sample. The error bars are the 68% confidence intervals.

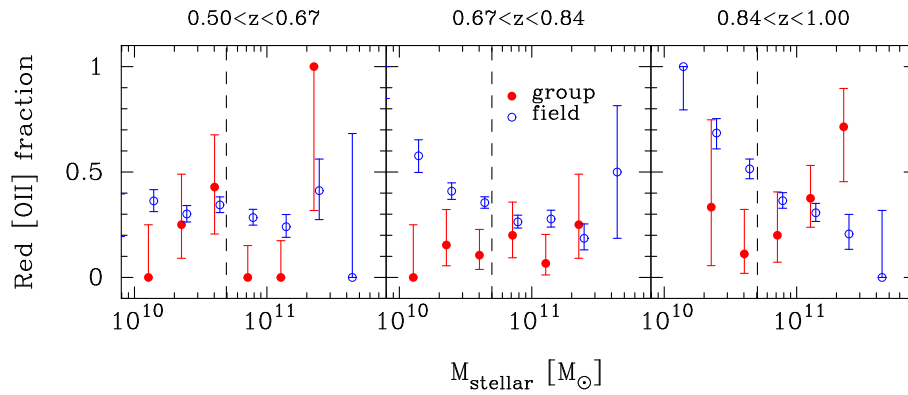


**Fig. 5.** Fraction of red [OII] emitters as a function of stellar mass. As in Fig. 4, the panels are split into the three redshift bins. The vertical dashed lines are the stellar mass cuts. The error bars are the 68% confidence intervals.

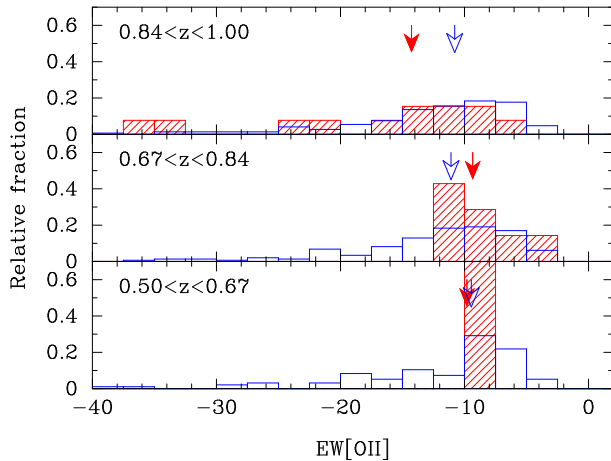


**Fig. 6.** Distribution of EW[OII] of red galaxies measured at  $> 2.3\sigma$  in groups (shaded histogram) and in the field (open histogram) environments based on the stellar mass limited sample. The arrows point the median of the EW[OII] in each environment.

tivities and the rates at which environment suppresses such activities are different in different environments. We will pursue this point in the next section.

## 4. Discussions

### 4.1. Comparisons with previous studies

Recent large spectroscopic surveys such as zCOSMOS (Lilly et al. 2007), DEEP2 (Davis et al. 2003), and VVDS (Le Fèvre et al. 2005) have enabled statistical analysis of galaxies in the universe up to  $z = 1$  and even beyond. Several authors have studied the environmental dependence of galaxy properties using data from those surveys (e.g., Cucciati et al. 2006; Cooper et al. 2007; Gerke et al. 2007; Cooper et al. 2010; Cucciati et al. 2010; Iovino et al. 2010). But, the results from those papers are not always consistent. In particular, results on the color-density relation at  $z \sim 1$  and interpretations of it seem to be controversial.

In fact, our finding that the fraction of red galaxies depends on environment up to  $z \sim 1$  does not seem to be consistent at a first glance with those from Cucciati et al. (2010) and Iovino et al. (2010) who have found no strong dependence of galaxy colors on density at  $z \sim 1$  based on a stellar mass limited sample. Another finding by Iovino et al. (2010) that the red fraction decreases with increasing redshift is not consistent either. Cooper et al. (2010) discussed differences in the data sets and in the ways analyses were made in the literature. But, we use basically the same data set as Cucciati et al. (2010) and Iovino et al. (2010) and the observed differences appear at odds. Here



we attribute the cause of the differences to differences in (i) definitions of environments and in (ii) definitions of red galaxies.

There is a fair amount of evidence that galaxy properties depend on the mass of groups and clusters at high redshifts (e.g., Tanaka et al. 2005; Poggianti et al. 2006; Koyama et al. 2007). In this paper, we use X-ray selected groups, while most of the previous papers from large spectroscopic surveys are based on galaxy groups (or galaxy densities) identified using spectroscopically observed galaxies. There are pros and cons in these environment definitions, but the advantage of the X-ray groups is that our environment is mass-selected. As mentioned earlier, 90% of the groups at  $z < 1$  in COSMOS are spectroscopically confirmed, and we probably sample the group-mass environments well in this study. A further comparison between optical and X-ray groups will be made in Finoguenov et al. (in prep).

A disadvantage would be that we cannot identify very low-mass groups which are below our X-ray detection limit, while optical group identification algorithms can. We suspect that these low-mass groups would be the primary cause of the difference from Cucciati et al. (2010) and Iovino et al. (2010). Iovino et al. (2010) showed that optically poor groups tend to exhibit a lower red fraction than optically rich groups. Poor groups are more numerous than rich ones and they dominate the group sample, which results in a smaller difference in the red fraction between groups and field. The difference in the group mass ranges explored could account for the difference in the dependence of the red fraction on environment between us and the previous studies. We note that George et al. (2011) recently observed clear dependence of the red fraction as a function of stellar mass on environment based on the photometric data in COSMOS.

Another cause of the difference is that our definition of red galaxies is different from that adopted in Iovino et al. (2010). They adopted a color threshold of  $U - B = 1$  regardless of redshift and stellar mass of galaxies, while we account for the tilt of the red sequence with respect to stellar mass and also for the passive evolution. We have confirmed that the red fraction decreases at higher redshifts if we adopt the same definition as theirs. We prefer to account for the tilt and passive evolution to define red/blue galaxies in this paper. The above two reasons are likely the primary causes of the somewhat different results between us and the previous authors.

Gerke et al. (2007) and Cooper et al. (2007) also suggested that the red fraction decreases with increasing redshifts in high density environments. This might be due to the selection of galaxies. They applied a rest-frame  $B$ -band magnitude cut, not a stellar mass cut. The  $B$ -band magnitude cut introduces a strong bias towards star forming galaxies, which could result in a lower red fraction at higher redshifts.

We note that there is a non-zero possibility that we are missing groups dominated by blue galaxies because we used the red sequence finder in the group identification process and that could possibly enhance the difference between groups and field. However, our technique uses a contrast of the red sequence between group and field and we do not actually require a higher fraction of red galaxies in groups. Even if groups had the same red fraction as the field, we can identify them as long as they show an over-density. We miss only groups in which

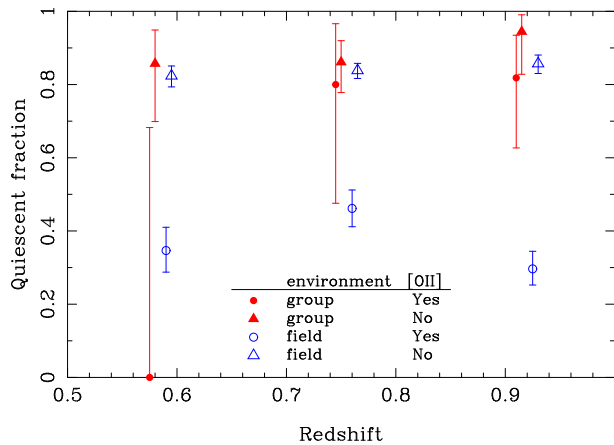


**Fig. 7.** Fraction of quiescent galaxies with  $(NUV - r)_{dered} > 3.5$  among the red galaxies in groups and field with/without [OII] plotted against redshift. The meanings of the symbols are shown in the plot. The error bars show the 68% confidence intervals.

the fraction of red galaxies is significantly lower than the field. It is unlikely that such very blue groups are so abundant that they change our results significantly because we have identified  $\sim 90\%$  of all the X-ray group candidates at  $z < 1$  with high significance and they exhibit a clearer red sequence compared to field galaxies.

Recently, Koyama et al. (2011) reported on  $H\alpha$  narrow-band imaging of a  $z = 0.4$  cluster. They found that groups exhibit a higher fraction of  $H\alpha$  emitters than in the field, which is in contrast to our finding in the right panel of Fig. 3. There are a number of differences in the explored stellar mass range, observing technique, emission line used and emission line sensitivity. These differences hinder detailed comparisons with our results.

#### 4.2. Origin of the [OII] emission – star formation vs AGN

The increasing fraction of red [OII] emitters with increasing redshift must be due to increasing dusty star formation activities and/or AGN activities. Recent studies of  $z > 1$  clusters also reported on increased rate of emission line galaxies in clusters than in lower redshift clusters (e.g., Hayashi et al. 2010, but see also Bauer et al. 2011). But, this trend is not established yet, and it is not clear if the emission line originates from star formation or AGN activities either.

Let us first ask if the [OII] emission is due to dusty star formation. We look at the  $(NUV - r)_{dered}$  color of the [OII] emitters taken from Ilbert et al. (2009). The  $(NUV - r)_{dered}$  color is a reddening corrected color of galaxy templates used for the photometric redshift estimates (i.e., the raw template colors without dust extinction) using the 30-band photometry. This is sensitive to on-going star formation as shown by Ilbert et al. (2010). We adopt a threshold of  $(NUV - r)_{dered} = 3.5$  to separate quiescent galaxies from star-forming galaxies (Ilbert et al. 2010) and plot the fraction of quiescent galaxies in Fig. 7. As the color from Ilbert et al. (2009) is based on photometric redshifts, we use galaxies with correct photometric redshifts ( $|z_{phot} - z_{spec}| < 0.05$ ). We note that this analysis is essentially equivalent to the popular two-color diagnostics to separate qui-



escent red galaxies from dusty ones (Wolf et al. 2005; Wolf et al. 2009). But, instead of using only 2 colors, we here make use of the 30-band photometry that gives a fine sampling of galaxy SEDs over a wide wavelength range to discriminate quiescent galaxies from dusty star forming ones.

Let us start with the red galaxies without significant [OII] emission shown by the open and filled triangles. The quiescent fractions of these galaxies are very high as expected from the absence of [OII]. The stellar population of these galaxies is typically old and there is no significant difference between groups and field. That is, if red galaxies exhibit no [OII], they are dominated by old stellar populations regardless of environment. Now, we turn our attention to the red [OII] emitters. The quiescent fraction of the red [OII] emitters in the field (open circle) is relatively low (30 – 40%), suggesting that more than a half of them are not quiescent and are probably undergoing dusty star formation. In contrast, the red [OII] emitters in groups (filled circle) show a very high quiescent fraction even at high redshifts and it is as high as those without [OII] emission. This suggests that red [OII] emitters in groups are dominated by old stellar populations despite the [OII] emission. In Fig. 3, we observed a sharp increase in the fraction of red [OII] emitters in high redshift groups, but the quiescent fraction does not show a corresponding decrease. There is no clear evidence for increased dusty galaxies in the red [OII] emitters in groups. Instead, Fig. 7 favors the AGN origin.

Let us then stand on the other side of the view and ask whether the [OII] emission comes from AGNs. At the redshift range under study, we cannot use strong emission line diagnostics such as the one proposed by Baldwin et al. (1981) to identify AGNs as the  $H\alpha$  line migrates to near-IR. Here we take another way to identify AGNs – X-rays – and quantify how AGNs populate in the redshift range studied here. We use the Chandra point source catalog (Elvis et al. 2009) and apply an X-ray luminosity cut of  $L_{0.5-10\text{keV}} > 10^{43} \text{ erg s}^{-1}$ , at which we are nearly complete up to  $z = 1$ . In the field, an X-ray detection rate of the red [OII] emitters seems to increase in the highest redshift bin:  $0.04 \pm 0.03$ ,  $0.03 \pm 0.02$ , and  $0.13 \pm 0.04$  from low to high redshift bins. However, we detect no red [OII] emitters in groups in X-rays:  $0.00^{+0.68}_{-0.00}$ ,  $0.00^{+0.32}_{-0.00}$ , and  $0.00^{+0.17}_{-0.00}$  from low to high redshifts.

Most of the red [OII] emitters in groups are not detected in X-rays (only 2 are detected, but with luminosities below the cut applied above). Tanaka et al. (2011) found that AGNs in quiescent galaxies are typically soft, low-luminosity AGNs in the local universe. Motivated by this, we performed a stacking analysis of those undetected sources in the soft band with a special care to remove the extended component (Finoguenov et al. 2009). By stacking 9 objects that are not individually detected, we measure an average luminosity of  $2.8 \times 10^{-17} \text{ erg s}^{-1} \text{ cm}^{-2}$  in 0.5–2 keV, which translates into  $2.7 \times 10^{40}$  and  $1.5 \times 10^{41} \text{ erg s}^{-1}$  at  $z = 0.5$  and  $z = 1$ , respectively. This luminosity level can be explained both by low-luminosity AGN and star formation origins. We cannot constrain the AGN fraction in groups with X-rays.

X-rays unfortunately do not put any constraint on the AGN or dusty star formation origin, but the robust photometric analysis based on the 30 photometric bands presented above seems to lend support to the AGN origin of the [OII] emission, al-

though the statistics is poor. The stellar population of the red [OII] emitters in groups is old and there is no hint of strong on-going star formation in those galaxies. The observed [OII] emission is unlikely due to star formation and the most probable origin of it is AGNs.

A possibility of weak AGNs in groups is supported by recent work by Lemaux et al. (2010), who performed near-IR spectroscopy of galaxies dominated by old stellar population but have [OII] emission in  $z = 0.8$  and  $0.9$  clusters. They found that a significant fraction of them ( $\sim 70\%$ ) harbor AGNs. It would not be surprising if a large fraction of the red [OII] emitters in our high redshift groups are AGNs as they have similar photometric properties as those studied in Lemaux et al. (2010). However, other authors reported on increased dusty star formation activities in groups at high redshifts (e.g., Koyama et al. 2008; Koyama et al. 2010; Kocevski et al. 2011). Tanaka et al. (2009) found that group galaxies at  $z \sim 1.2$  show weak  $H\delta$  absorptions and they speculated that it might be due to large extinction. Post-starburst galaxies might favor groups (Poggianti et al. 2009). Vergani et al. (2010) also reported that post-starburst galaxies prefer high density environments based on the zCOSMOS data. Recently, Hayashi et al. (2011) observed that both AGN and star formation take place in a  $z = 1.4$  cluster.

Given this controversial situation, it is probably fair to say that the origin of the emission line is still unclear at this point. It may be that both dusty star formation activities and AGN activities increases at high redshifts and there is a strong cluster-cluster variation. Any conclusion on the origin of the [OII] emission needs to be drawn from a larger statistical sample of groups at  $z \gtrsim 1$ . An extensive near-IR spectroscopy targeting  $H\alpha$  and [NII] lines of the red [OII] emitters in groups to perform emission line diagnostics such as the one proposed by Baldwin et al. (1981) would be an obvious way forward. Also, the newly developed AGN identification method by Tanaka et al. (2011) is effective as well because it requires only [OII] and/or [OIII]. Deep Chandra observations are obviously helpful as well. Using these techniques, we first have to discriminate AGNs from star formation in order to interpret the recent observations that distant groups and clusters tend to show an increased rate of emission line galaxies.

## 5. Summary

We have presented photometric and spectroscopic analyses of zCOSMOS galaxies at  $0.5 < z < 1$ . Unlike most of the previous studies, we define the mass-selected environments to study the dependence of galaxy properties on environment. This is the most important feature of this work. Previous studies have shown that galaxy properties depend on mass of groups and clusters. These studies clearly show that environment needs to be defined by mass.

We have found that the fraction of red galaxies is always higher in groups than in the field at  $0.5 < z < 1$  and it does not strongly change over this redshift range. This result might appear inconsistent with previous studies from zCOSMOS, but we have argued that this is due to different environment definitions and to different definitions of red galaxies. The most important finding of this paper is that the fraction of [OII] emit-

ters on the red sequence increases in groups at higher redshifts, while the fraction does now show any significant evolution in the field. The increased red [OII] emitters in groups must be due to increased dusty star formation activities and/or to increased AGN activities. We have studied these two possibilities by using the 30-band photometry and X-ray data. While the X-ray data do not put a strong constraint on them, the 30-band photometry suggests that the stellar population of the [OII] emitters in groups is old and there is no hint of enhanced dusty star forming activities. This lends support to increased AGN activities.

Recent observations often report a high fraction of emission line galaxies in distant groups and clusters. The question now is where the emission comes from. We have obtained evidence for the AGN origin and recent near-IR spectroscopic work also favors it. But, our overall statistics is poor and some of the previous studies seem to favor the dusty star formation origin. More observations are obviously needed to settle the issue.

This work is supported by World Premier International Research Center Initiative (WPI Initiative), MEXT, Japan and also in part by KAKENHI No. 23740144. This work is based on observations undertaken at the European Southern Observatory (ESO) Very Large Telescope (VLT) under the Large Program 175.A-0839. We would like to thank the anonymous referee for useful comments, which helped improve the paper.

## References

- Aihara, H., et al. 2011, *ApJS*, 193, 29
- Baldwin, J. A., Phillips, M. M., & Terlevich, R. 1981, *PASP*, 93, 5
- Balogh, M. L., Morris, S. L., Yee, H. K. C., Carlberg, R. G., & Ellingson, E. 1997, *ApJL*, 488, L75
- Bauer, A. E., Grützbauch, R., Jørgensen, I., Varela, J., & Bergmann, M. 2011, *MNRAS*, 411, 2009
- Baldry, I. K., Balogh, M. L., Bower, R. G., Glazebrook, K., Nichol, R. C., Bamford, S. P., & Budavari, T. 2006, *MNRAS*, 373, 469
- Balogh, M. L., et al. 2011, *MNRAS*, 412, 2303
- Bielby, R. M., Finoguenov, A., Tanaka, M., et al. 2010, *A&A*, 523, A66
- Blanton, M. R., et al. 2003, *ApJ*, 594, 186
- Blanton, M. R., Eisenstein, D., Hogg, D. W., Schlegel, D. J., & Brinkmann, J. 2005, *ApJ*, 629, 143
- Bruzual, G., & Charlot, S. 2003, *MNRAS*, 344, 1000
- Bolzonella, M., et al. 2010, *A&A*, 524, A76
- Carlberg, R. G., Yee, H. K. C., & Ellingson, E. 1997, *ApJ*, 478, 462
- Chabrier, G. 2003, *PASP*, 115, 763
- Finoguenov, A., et al. 2007, *ApJS*, 172, 182
- Colless, M., et al. 2003, *arXiv:astro-ph/0306581*
- Cooper, M. C., et al. 2010, *MNRAS*, 409, 337
- Cooper, M. C., et al. 2007, *MNRAS*, 376, 1445
- Cucciati, O., et al. 2006, *A&A*, 458, 39
- Cucciati, O., et al. 2010, *A&A*, 524, A2
- Davis, M., et al. 2003, *Proc. SPIE*, 4834, 161
- Demarco, R., et al. 2005, *A&A*, 432, 381
- Demarco, R., et al. 2007, *ApJ*, 663, 164
- Doi, M., et al. 2010, *AJ*, 139, 1628
- Dressler, A. 1980, *ApJ*, 236, 351
- Dressler, A., et al. 1997, *ApJ*, 490, 577
- Elvis, M., et al. 2009, *ApJS*, 184, 158
- Fassbender, R., Böhringer, H., Lamer, G., Mullis, C. R., Rosati, P., Schwope, A., Kohnert, J., & Santos, J. S. 2008, *A&A*, 481, L73
- Finoguenov, A., et al. 2009, *ApJ*, 704, 564
- Finoguenov, A., et al. 2010, *MNRAS*, 403, 2063
- Fukugita, M., Ichikawa, T., Gunn, J. E., Doi, M., Shimasaku, K., & Schneider, D. P. 1996, *AJ*, 111, 1748
- Gehrels, N. 1986, *ApJ*, 303, 336
- Geller, M. J., & Huchra, J. P. 1989, *Science*, 246, 897
- George, M. R., Leauthaud, A., Bundy, K., et al. 2011, *arXiv:1109.6040*
- Gerke, B. F., et al. 2007, *MNRAS*, 376, 1425
- Gómez, P. L., et al. 2003, *ApJ*, 584, 210
- Goto, T., Yamauchi, C., Fujita, Y., Okamura, S., Sekiguchi, M., Smail, I., Bernardi, M., & Gomez, P. L. 2003, *MNRAS*, 346, 601
- Guzzo, L., et al. 2007, *ApJS*, 172, 254
- Hasinger, G., et al. 2007, *ApJS*, 172, 29
- Hayashi, M., Kodama, T., Koyama, Y., Tanaka, I., Shimasaku, K., & Okamura, S. 2010, *MNRAS*, 402, 1980
- Hayashi, M., Kodama, T., Koyama, Y., Tadaki, K.-I., & Tanaka, I. 2011, *MNRAS*, 415, 2670
- Ilbert, O., et al. 2009, *ApJ*, 690, 1236
- Ilbert, O., et al. 2010, *ApJ*, 709, 644
- Iovino, A., et al. 2010, *A&A*, 509, A40
- Kauffmann, G., White, S. D. M., Heckman, T. M., Ménard, B., Brinchmann, J., Charlot, S., Tremonti, C., & Brinkmann, J. 2004, *MNRAS*, 353, 713
- Kocevski, D. D., Lemaux, B. C., Lubin, L. M., et al. 2011, *ApJL*, 737, L38
- Kodama, T., Smail, I., Nakata, F., Okamura, S., & Bower, R. G. 2001, *ApJL*, 562, L9
- Koekemoer, A. M., et al. 2007, *ApJS*, 172, 196
- Koyama, Y., Kodama, T., Tanaka, M., Shimasaku, K., & Okamura, S. 2007, *MNRAS*, 382, 1719
- Koyama, Y., et al. 2008, *MNRAS*, 391, 1758
- Koyama, Y., Kodama, T., Shimasaku, K., Hayashi, M., Okamura, S., Tanaka, I., & Tokoku, C. 2010, *MNRAS*, 403, 1611
- Koyama, Y., Kodama, T., Nakata, F., Shimasaku, K., & Okamura, S. 2011, *ApJ*, 734, 66
- Leauthaud, A., et al. 2010, *ApJ*, 709, 97
- Le Fèvre, O., et al. 2003, *Proc. SPIE*, 4841, 1670
- Le Fèvre, O., et al. 2005, *A&A*, 439, 845
- Lewis, I., et al. 2002, *MNRAS*, 334, 673
- Lemaux, B. C., Lubin, L. M., Shapley, A., Kocevski, D., Gal, R. R., & Squires, G. K. 2010, *ApJ*, 716, 970
- Lidman, C., et al. 2008, *A&A*, 489, 981
- Lilly, S. J., Le Fèvre, O., Crampton, D., Hammer, F., & Tresse, L. 1995, *ApJ*, 455, 50
- Lilly, S. J., et al. 2009, *ApJS*, 184, 218
- Lilly, S. J., et al. 2007, *ApJS*, 172, 70
- Lubin, L. M., Oke, J. B., & Postman, M. 2002, *AJ*, 124, 1905
- Mei, S., et al. 2009, *ApJ*, 690, 42
- Nakata, F., Bower, R. G., Balogh, M. L., & Wilman, D. J. 2005, *MNRAS*, 357, 679
- Rettura, A., et al. 2010, *ApJ*, 709, 512
- Rosati, P., Stanford, S. A., Eisenhardt, P. R., Elston, R., Spinrad, H., Stern, D., & Dey, A. 1999, *AJ*, 118, 76
- Strazzullo, V., et al. 2010, *arXiv:1009.1423*
- Poggianti, B. M., Smail, I., Dressler, A., Couch, W. J., Barger, A. J., Butcher, H., Ellis, R. S., & Oemler, A., Jr. 1999, *ApJ*, 518, 576
- Poggianti, B. M., et al. 2006, *ApJ*, 642, 188
- Poggianti, B. M., et al. 2008, *ApJ*, 684, 888
- Poggianti, B. M., et al. 2009, *ApJ*, 693, 112
- Postman, M., & Geller, M. J. 1984, *ApJ*, 281, 95
- Scoville, N., et al. 2007, *ApJS*, 172, 1

- Shectman, S. A., Landy, S. D., Oemler, A., Tucker, D. L., Lin, H.,  
Kirshner, R. P., & Schechter, P. L. 1996, *ApJ*, 470, 172
- Stanford, S. A., et al. 2005, *ApJL*, 634, L129
- Stanford, S. A., et al. 2006, *ApJL*, 646, L13
- Tanaka, M., Goto, T., Okamura, S., Shimasaku, K., & Brinkmann, J.  
2004, *AJ*, 128, 2677
- Tanaka, M., Kodama, T., Arimoto, N., Okamura, S., Umetsu, K.,  
Shimasaku, K., Tanaka, I., & Yamada, T. 2005, *MNRAS*, 362,  
268
- Tanaka, M., Lidman, C., Bower, R. G., Demarco, R., Finoguenov, A.,  
Kodama, T., Nakata, F., & Rosati, P. 2009, *A&A*, 507, 671
- Tanaka, M., Finoguenov, A., & Ueda, Y. 2010a, *ApJL*, 716, L152
- Tanaka, M., De Breuck, C., Venemans, B., & Kurk, J. 2010b, *A&A*,  
518, A18
- Tanaka, M. 2011, *PASJ* submitted.
- Tasca, L. A. M., et al. 2009, *A&A*, 503, 379
- Vergani, D., et al. 2010, *A&A*, 509, A42
- Whitmore, B. C., Gilmore, D. M., & Jones, C. 1993, *ApJ*, 407, 489
- Wilman, D. J., et al. 2008, *ApJ*, 680, 1009
- Wolf, C., Gray, M. E., & Meisenheimer, K. 2005, *A&A*, 443, 435
- Wolf, C., et al. 2009, *MNRAS*, 393, 1302
- York, D. G., et al. 2000, *AJ*, 120, 1579